Int. J. Multiphase Flow Vol. 19, No. 4, pp. 589–610, 1993
Printed in Great Britain.

0301-9322/93 $6.00 + 0.00

THE MOVING CONTACT LINE ON A SMOOTH SOLID SURFACE

Y. D. SHIKHMURZAEV
Institute of Mechanics, University of Moscow, 119899 Moscow, Russia

(Received 22 December 1991; in revised form 23 December 1992)

Abstract—A mathematical model for the advancing contact-line motion on a smooth solid surface is proposed. It is shown that in the spreading of liquids over solid surfaces, the flow causes a surface tension gradient along the liquid–solid interface which influences the flow and, in the case of small capillary and Reynolds numbers, determines the dynamic contact angle and the force between the liquid and solid in the vicinity of the contact line. The model: (a) eliminates the shear-stress singularity of the classical model; (b) describes the fluid motion as *rolling*, in complete agreement with direct experimental observations; (c) determines the dynamic contact angle and the tangential force dependence on the contact-line speed; (d) explains the existence of the maximum contact angle values $< 180°$; (e) predicts a contact-line instability and an incipient air entrainment. It is shown also that, in the case of small capillary numbers, the force experienced by the solid in the vicinity of the contact line is determined by the surface tension gradient along the liquid–solid interface and not by the shear stress. A relationship between the parameters of Young's equation and the limiting dynamic contact angle value is found and a new method for independent measurement of these parameters is proposed. Qualitative and quantitative comparison of the theory with the experimental data of various authors is carried out. The model could be used in the treatment of a number of coating and multiphase problems with moving contact lines on smooth surfaces and gives a sound basis for conventional models developed for rough surfaces.

Key Words: wetting, dynamic contact angle, shear-stress singularity, irreversible thermodynamics

1. INTRODUCTION

A contact line is formed at the intersection of a fluid–fluid interface and a solid. The contact-line motion is an important factor in many natural and various technological processes; among the latter, coating of solids by liquid films, tertiary oil recovery, wetting of powders, polymer processing, textile manufacturing, photographic film and magnetic disk production, chemical technologies and many others.

The present paper deals with the advancing contact-line problem, i.e. the motion of a liquid which displaces a gas from a solid surface. Experimental studies have revealed the following features of this phenomenon:

(i) The spreading of liquids over the surfaces of solids is *rolling* (Yarnold 1938; Dussan & Davis 1974; Ngan & Dussan 1982), i.e. the free surface velocity directed towards the contact line is greater than that in the bulk; material points initially located on the gas–liquid interface arrive at the solid surface in a finite interval of time.

(ii) The dynamic contact angle θ_d grows from the static value θ_s to some limiting value θ_{max} as the contact-line speed increases (Schonhorn *et al.* 1966; Inverarity 1969; Schwartz & Tejada 1972; Hoffman 1975; Gutoff & Kendrick 1982; Ström *et al.* 1990).

(iii) The value of θ_{max} depends on the contacting media (Schwartz & Tejada 1972) and, though most gas–liquid–solid systems have a limiting contact angle equal or very close to 180° (Inverarity 1969; Hoffman 1975; Ström *et al.* 1990), for some of them it is considerably less than 180° (Ablett 1923; Inverarity 1969; Elliott & Riddiford 1967; Schwartz & Tejada 1972).

(iv) At a certain contact-line speed, which depends on the materials of the system, an instability of the contact-line motion occurs which results in a "sawtooth"

form of the contact line and gas entrainment in the spreading liquid (Burley & Kennedy 1976a, b; Blake & Ruschak 1979; Gutoff & Kendrick 1982).

A mathematical modelling of the advancing contact-line problem encounters a fundamental difficulty. The classical formulation of the problem (Moffatt 1964) with the no-slip boundary condition on a solid surface gives rise to a non-integrable singularity of the shear stress, i.e. to an infinite force exerted by the fluid on the solid. The pressure of the fluid at the moving contact line is singular as well. These singularities are an immediate consequence of the multi-valuedness of the velocity field inherent in the classical solution, i.e. the value of the velocity vector at the contact line depends upon the direction from which it is approached (Batchelor 1967, p. 226; Dussan & Davis 1974). In the classical formulation the fluid motion is *rolling* [see feature (i)]; the dynamic contact angle value cannot be found and must be prescribed.

From a physical point of view, the non-integrable shear-stress singularity is absolutely unacceptable, and the formulation of the problem must be altered in such a way that the singularity is removed. The main approach which is used to eliminate the shear-stress singularity is to replace the no-slip boundary condition on the solid surface by a slip one (Huh & Scriven 1971; Hocking 1976, 1977; Dussan 1976; Neogi & Miller 1976; Huh & Mason 1977; Greenspan 1978; Lowndes 1980; Durbin 1988; Baiocchi & Pukhnachev 1990). The contact angle is defined as the angle between two boundaries on which the boundary conditions for the fluid motion are formulated. The most popular boundary condition is the linear slip–shear relation (Lamb 1932, p. 586), with different expressions for the slip coefficient due to different physical backgrounds.

In order to justify this boundary condition, Hocking (1976) proposed that on a scale of surface roughness the slip does not occur. The gas–liquid interface laying down on surface roughness elements produces the appearance of slip and of the contact-line motion. This scheme allows one to find the relationship between the macroscopic slip coefficient and the microscopic structure of a solid surface. Though the model does not describe the wetting process on the microscopic length scale, the approach itself is very interesting, since for sufficiently rough surfaces and high speeds of liquid spreading it presents a picture of macroscopic "wetting" of the "effective" plane surface. This approach, completed using the model suitable to the scale of surface roughness, in principle, could give the model applicable for surfaces of arbitrary roughness and arbitrary rates of wetting.

A model attributing the slip to the surface roughness was proposed also by Neogi & Miller (1976).

In the paper of Huh & Mason (1977), the slip boundary condition is based on a physical model of the gas–liquid interface motion. According to this model, the molecules which arrive at the contact line are not oriented and require a finite interval of time to attach themselves to the solid surface. On the length proportional to this interval of time and the contact-line speed they experience no drag force and after attaching themselves do not slip along the surface. The idea of relaxation seems very perspective, though, as it was pointed out by Dussan (1979) that: the argumentation of the model declares that the liquid undergoes a *rolling* motion, but the solution of the problem shows that for the boundary conditions described above it is not so. The formulation of Huh & Mason leads to an integrable singularity on the solid boundary and is equivalent to some special relative-velocity distribution.

Durbin (1988) proposed that the slip occurs as a consequence of a direct limitation of the maximum shear-stress density. This yield stress is attributed to the breaking of cohesive bonds between the bulk of the liquid and an adsorbed surface layer.

Baiocchi & Pukhnachev (1990) assumed that the relative-velocity distribution is the one which minimizes the entropy production in the vicinity of a moving contact line. The analysis carried out in their paper allowed them to obtain this distribution.

The description of the dynamic contact angle dependence on the contact-line speed has been studied intensively during the last 20 years. Generally, in the vicinity of the contact line the gas–liquid interface is approximated by a plane surface with a prescribed angle between this surface and the solid one. This contact angle, which can be called the *macroscopic* one (since it is used as the boundary condition for the macroscopic hydrodynamic equation determining the free surface shape), is usually assumed to be equal to the static one, even for non-zero contact-line speed (Lowndes 1980; Hocking & Rivers 1982; Cox 1986; Baiocchi & Pukhnachev 1990). Far from

the contact line the free surface shape is deformed by viscous stresses and one may introduce an *apparent* contact angle—the angle formed by free and solid surfaces far from the contact line. Assuming this *apparent* contact angle to be the angle measured in experiments, many authors (Lowndes 1980; Hocking & Rivers 1982; Cox 1986; Zhou & Sheng 1990; and others) obtained good agreement between the models and some experiments. Relations between *macroscopic* and *apparent* contact angles and some aspects of the comparison of experiments to theory were discussed by Ngan & Dussan (1982, 1989).

The recent results of Zhou & Sheng (1990) show, however, that the relation between measured and *apparent* contact angles is not so simple and a (non-trivial) dependence of the *macroscopic* contact angle on the contact-line speed requires further investigation. It is also difficult to understand how the limiting *apparent* contact angle could be $<180^\circ$ [see feature (iii)], since it is measured *far* from the contact line and, therefore, should be independent of the solid surface material.

It is necessary to mention that not only the *apparent* contact angle but also the *macroscopic* one may differ from the so-called *actual* or *microscopic* contact angle: in some cases the liquid which spreads over a solid surface is preceded by a thin *precursor* film (Hardy 1919; Bascom *et al.* 1964) which forms its own, *actual*, contact angle with the solid surface. Thus, when introducing the concept "contact angle" one should specify the manner of its application. As will be shown below, the main role in the description of the hydrodynamic characteristics of wetting phenomena belongs to the *macroscopic* contact angle.

The works of Voinov (1976, 1978) and Boender *et al.* (1991) differ from the ones cited above, since they do not consider the problem of a non-integrable stress singularity, attributing it to non-continuum effects at a distance of the order of a molecular dimension. Using the no-slip condition on the solid boundary and some assumptions concerning the immediate vicinity of the contact line, Voinov and Boender *et al.* obtained the long-range asymptotics of the free surface shape in fairly good agreement with some experiments.

The principal objective of the present paper is to develop an approach to the problem which eliminates the singularities of the classical model and describes features (i)–(iv) of the phenomenon. The main idea of this approach is very simple and can be explained as follows. Since, in the advancing contact-line motion, material elements move from a free surface to the solid surface [see feature (i)], their properties gradually change—asymptoting to the equilibrium properties of the liquid–solid interface. Thus, *the flow itself* causes a surface tension gradient along the liquid–solid interface which has a reverse influence upon the flow and, in particular, influences the dynamic contact angle and the force between the liquid and the solid in the vicinity of the contact line. One variant of the mathematical model representing this approach is given in section 2. In section 3 the problem for small capillary numbers (Ca) is formulated, and in section 4 it is simplified using the technique of matched asymptotic expansions. Section 5 presents a numerical analysis of the problem in the case of small Ca and a qualitative comparison of the results with experimental observations. In section 6 the theory is compared quantitatively with the experimental data of different authors. In section 7 we summarize the main results of the work and discuss the possibilities for its generalization and its relations with other models. In section 7 we also discuss a way to combine the present approach with one of the models developed previously for rough surfaces, which could give a general model applicable to surfaces of arbitrary roughness.

2. MODEL

Let us consider an isothermal displacement of an inviscid gas by a Newtonian liquid which spreads on a smooth solid surface. Our analysis is restricted to small Ca and Re (Reynolds number). We consider the vicinity of the contact line, with characteristic dimensions less than the lengthscales of the flow field (the dimension of a spreading drop, liquid film thickness, capillary gap etc.) and large in comparison with the thickness of the interfacial layer, in which the physical characteristics of the liquids differ strongly from those of the bulk. Thus, we may consider the flow field in a wedge region, substituting gas–liquid and solid–liquid interfacial layers for interfacial surfaces of zero thickness. The structure of a three-phase interaction region (called also the contact line) deserves

special attention and will be discussed below. The interfaces can possess some intrinsic, "surface", properties (e.g. surface tension) which play an important role in the hydrodynamics of wetting. The component of fluid velocity parallel to the contact line is assumed to be absent.

In an advancing contact-line motion, the liquid particles which initially form an element of the gas–liquid interface (e.g. AB, Fig. 1) in a finite time arrive on the solid surface and form an element of the solid–liquid interface (A′B′, Fig. 1). During this process the surface properties of this element change from the equilibrium surface properties of the free surface to those of the liquid–solid interface. It is evident that this change in the surface properties is not instantaneous: it is a result of some transitional process with its specific kinetics dependent on the properties of the contacting materials. The finiteness of the surface tension relaxation time gives rise to the formation of regions with large surface tension gradients, which can considerably influence the whole motion of the liquid in the vicinity of the contact line. Guided by this consideration, we are going to derive the governing equations for the kinetics of the surface tension relaxation process.

2.1. Surface thermo- and hydrodynamics of the relaxation process

Before deriving the governing equations of the relaxation process and its relationship with the motion in the bulk, let us formulate the main idea of this derivation. It is well-known from experiments that the surface tension is a function of temperature (Daniels & Alberty 1975). These experiments deal with the *equilibrium* surface tension which depends on the *pair of contacting materials*. Physically this dependence is due to the specific position of the interface molecules, which experience different intermolecular forces from molecules of the bulk phases. From a macroscopic point of view, this means that the surface tension is a function of the other surface parameters (besides temperature), and the structure of intermolecular forces from the bulk phases determines the *equilibrium* values of these parameters. For example, one may choose the surface density, concentrations of surfactants and some other quantities as the surface constitutive parameters.

We will consider the simplest case in which the surface tension depends only on temperature T and one more surface parameter, namely, the surface density ρ^s. If the surface density is not singular (Adam 1930; Defay & Prigogine 1966), i.e. it is small in comparison with the bulk density multiplied by the (macroscopic) length characteristic for the flow field, the inertial properties of the interface are negligible but the changes in the surface density govern (in the isothermal case) the surface tension relaxation process. Thus, the surface tension relaxation implies mass exchange between the interfaces and the bulk. It is worth mentioning that the idea of the liquid–solid interface formation due to the mass flux into it from the bulk has been already considered on the basis of the equations of chemical kinetics by Blake & Haynes (1969). They have found good agreement between their results and experimental data, but the hydrodynamic aspects of the problem (i.e. the shear stress singularity) were not considered in their paper.

Two main macroscopic approaches to the derivation of the surface hydrodynamics equations may be distinguished. The first, "structural", considers the interface as a layer of finite thickness using the continuum mechanics equations for its description. The characteristic thickness of the interfacial layer corresponds to the range of intermolecular forces which play the main role in making this layer a specific, "surface", phase (Rowlinson & Widom 1982). The distributions of parameters in this layer and in the bulk must be matched asymptotically. "Surface" parameters may be introduced as a result of the averaging of the corresponding volumetric parameters across the layer and, obviously, they should not be matched with the bulk parameters. In principle, this approach allows one to obtain equations applicable for arbitrary deviations of the system from equilibrium and also the transport coefficients. In the case of very small dimensions of the flow domain (e.g. for the spreading of droplets of about 10^{-8} m dia) the application of the "structural" approach is the only possibility and it leads to encouraging results [see de Gennes (1985) for a review]. It is necessary to emphasize that the dynamic contact angle obtained by means of this approach is the *actual* one (see section 1). It is necessary to mention also that our knowledge of the structure of the intermolecular forces which act between the surface layer and the bulk is far from complete and this fact leads to some difficulties in applications of this approach (Heslot *et al.* 1989), especially in the case of finite contact angle values (de Gennes *et al.* 1990). However, the representation of the interface as a layer of finite thickness is convenient for the order-of-magnitude analysis and for the illustration of the results obtained by other methods.

If the characteristic dimensions of the flow domain are not so small, one may use another, "structureless", approach which is simpler than the "structural" one. This approach considers the interface as a geometrical surface with intrinsic, "surface", properties (Bedeaux *et al.* 1976). The main problem in this approach is to describe the mass, momentum and energy exchange between the interface and the bulk, since the nature and structure of intermolecular forces are not considered explicitly. If the deviation from equilibrium is not large, one may assume the fluxes of mass, momentum and energy to be proportional to the deviations of the surface parameters from their equilibrium values. However, this simplification leads to a number of unknown phenomenological coefficients which should be obtained experimentally or by means of a detailed analysis of the interface structure.

In the present paper, for the derivation of the surface hydrodynamics equations we employ the method of the thermodynamics of irreversible processes in the framework of the "structureless" approach using the mathematical technique and some results of Bedeaux *et al.* (1976). We will also use the representation of the interface as a layer of finite thickness for the order-of-magnitude analysis.

Since we are not interested in the consideration of a gas or a solid in the study of the advancing contact-line problem, it is convenient to carry out the derivation in the following way. We will consider a system of two immiscible fluids (I and II), assuming that the interface is formed by molecules *of only one of them* (fluid I), and obtain the required equations using the limits of zero and infinite viscosity of fluid II for the gas–liquid and solid–liquid interfaces, respectively. The case of a *real* fluid–fluid system, in which the interface consists of molecules of *both* fluids, is more difficult and can be found elsewhere (Shikhmurzaev 1993a).

Taking into account this remark, we now consider the fluid–fluid system with a moving interface $\Sigma(t)$ which is defined by $f(\mathbf{r}, t) = 0$, such that $f(\mathbf{r}, t) > 0$ refers to points in fluid I (the future liquid) and $f(\mathbf{r}, t) < 0$ refers to points in fluid II (the future solid or gas). Following Bedeaux *et al.* (1976), we introduce some functions and their properties:

$$\theta^+(f) \equiv \begin{cases} 1, & f > 0 \\ 0, & f \leqslant 0 \end{cases}, \qquad \theta^-(f) \equiv \begin{cases} 0, & f \geqslant 0 \\ 1, & f < 0 \end{cases}, \qquad \frac{\partial \theta^{\pm}(f)}{\partial f} = \pm\delta(f);$$

$$\mathbf{n} = \frac{\operatorname{grad} f}{|\operatorname{grad} f|}, \quad \text{if } f = 0, \qquad \frac{\partial f}{\partial t} = -\mathbf{v}^{\mathrm{s}} \cdot \operatorname{grad} f = -v_{\mathrm{n}}^{\mathrm{s}} |\operatorname{grad} f|, \quad \text{if } f = 0;$$

$$\delta^{\mathrm{s}}(\mathbf{r}, t) \equiv |\operatorname{grad} f(\mathbf{r}, t)|\, \delta(f(\mathbf{r}, t)), \frac{\partial}{\partial \mathbf{r}} \theta^{\pm}(f(\mathbf{r}, t)) = \pm \mathbf{n} \delta^{\mathrm{s}}(\mathbf{r}, t);$$

$$\frac{\partial}{\partial t} \theta^{\pm}(f(\mathbf{r}, t)) = \mp v_{\mathrm{n}}^{\mathrm{s}} \delta^{\mathrm{s}}(\mathbf{r}, t), \qquad \frac{\mathrm{d}^{\mathrm{s}}}{\mathrm{d}t} \equiv \frac{\partial}{\partial t} + \mathbf{v}^{\mathrm{s}} \cdot \operatorname{grad}, \qquad \frac{\mathrm{d}^{\mathrm{s}} f}{\mathrm{d}t} = 0 \quad \text{if } f = 0;$$

$$\frac{\mathrm{d}^{\mathrm{s}}}{\mathrm{d}t} \theta^{\pm}(f) = 0, \qquad \frac{\mathrm{d}^{\mathrm{s}}}{\mathrm{d}t} \delta^{\mathrm{s}} = 0. \qquad [1]$$

Here $\theta^{\pm}$ are the Heaviside functions; δ and δ^{s} are delta and "surface" delta functions, respectively; $\mathbf{n}$ is the normal to the surface which points from fluid II to fluid I; and $v_{\mathrm{n}}^{\mathrm{s}}$ is the normal component of the interface velocity; the parallel components of $\mathbf{v}^{\mathrm{s}}$ will be defined below.

Let us consider the conservation laws of mass and momentum, introducing the following quantities defined for all values of $\mathbf{r}$:

$$\rho = \rho^+(\mathbf{r}, t)\theta^+(f) + \rho^{\mathrm{s}}\delta^{\mathrm{s}} + \rho^-(\mathbf{r}, t)\theta^-(f); \qquad [2]$$

$$\mathbf{g} = \rho \mathbf{v} = \rho^- \mathbf{v}^- \theta^- + \rho^{\mathrm{s}} \mathbf{v}^{\mathrm{s}} \delta^{\mathrm{s}} + \rho^+ \mathbf{v}^+ \theta^+, \quad \mathbf{v} \equiv \begin{cases} \mathbf{v}^+ & \text{if } f > 0 \\ \mathbf{v}^{\mathrm{s}} & \text{if } f = 0 \\ \mathbf{v}^- & \text{if } f < 0 \end{cases}; \qquad [3]$$

and

$$\mathbf{P} = \mathbf{P}^- \theta^- + \mathbf{P}^{\mathrm{s}} \delta^{\mathrm{s}} + \mathbf{P}^+ \theta^+, \quad \mathbf{gv} = \mathbf{g}^+ \mathbf{v}^+ \theta^+ + \mathbf{g}^- \mathbf{v}^- \theta^- + \mathbf{g}^{\mathrm{s}} \mathbf{v}^{\mathrm{s}} \delta^{\mathrm{s}}. \qquad [4]$$

Here ρ, $\mathbf{v}$, $\mathbf{g}$, $\mathbf{P}$ and $\mathbf{gv}$ are the density, velocity, momentum density, stress tensor and convective component of the moment flux, respectively. These quantities coincide with the corresponding

quantities of fluid I (superscript +) in the region where $f > 0$ and those of fluid II (superscript −) if $f < 0$. The superscript s indicates the quantities which are only defined on the surface; the normal derivatives of these quantities as well as those of the vector $\mathbf{n}$ are equal to zero.

Substituting [2] and [3] into the continuity equation and taking into account the properties of generalized functions [1], as well as the condition that the coefficients of θ^+, θ^- and δ^s are separately zero, we obtain the continuity equations for the bulk phases and for the interface. The continuity equations in the bulks have their usual form and for the interface (which consists only of the molecules of fluid I, i.e. $v_n^- - v_n^s = 0$), this may be written as

$$\frac{\partial \rho^s}{\partial t} + \operatorname{div} \rho^s \mathbf{v}^s = -\rho^+ (v_n^+ - v_n^s). \tag{5}$$

The analogous procedure carried out with the momentum balance equation, considering the fact that the coefficients of δ^s and the normal component of the coefficient of $(\partial/\partial \mathbf{r})\delta^s$ are separately zero (Bedeaux *et al.* 1976), gives the usual momentum balance equations in the bulks and the following equalities for the surface parameters:

$$\mathbf{n} \cdot \mathbf{P}^s = 0 \tag{6}$$

and

$$\frac{\partial \mathbf{g}^s}{\partial t} + \operatorname{div} \mathbf{g}^s \mathbf{v}^s + \rho^+ \mathbf{v}^+ (v_n^+ - v_n^s) = \operatorname{div} \mathbf{P}^s + \mathbf{n} \cdot (\mathbf{P}^+ - \mathbf{P}^-). \tag{7}$$

The latter equation for the non-singular surface density ρ^s (i.e. if $\rho^s \ll \rho^+ \cdot L$, where L is the lengthscale of the flow domain) takes the form of a known generalized equation of capillarity:

$$\operatorname{div} \mathbf{P}^s + \mathbf{n} \cdot (\mathbf{P}^+ - \mathbf{P}^-) = 0. \tag{8}$$

Now we will consider the conservation of energy and construct relations which define the mass, momentum and energy fluxes between the interface and the bulks. We define the energy per unit volume e_v, the energy current $\mathbf{J}_e$ and the heat current $\mathbf{J}_q$ as

$$e_v = e_v^+ \theta^+ + e_v^s \delta^s + e_v^- \theta^-, \quad \mathbf{J}_e = \mathbf{J}_e^+ \theta^+ + \mathbf{J}_e^s \delta^s + \mathbf{J}_e^- \theta^- = -\mathbf{P} \cdot \mathbf{v} + e_v \mathbf{v} + \mathbf{J}_q.$$

The energy conservation equation for the surface phase takes the form

$$\frac{\mathrm{d}^s e_v^s}{\mathrm{d}t} = -e_v^s \operatorname{div} \mathbf{v}^s + \operatorname{div}(\mathbf{P}^s \cdot \mathbf{v}^s) - \operatorname{div} \mathbf{J}_q^s + \mathbf{n} \cdot (\mathbf{P}^+ \cdot \mathbf{v}^+ - \mathbf{P}^- \cdot \mathbf{v}^-)$$
$$- (\mathbf{J}_{q,n}^+ - \mathbf{J}_{q,n}^-) - e_v^+ (v_n^+ - v_n^s). \tag{9}$$

In contrast to Bedeaux *et al.*, we will consider the one-temperature model (close to the interface $T^+ = T^- = T^s = T$); the main emphasis being on the influence of the surface density changes on the surface phase hydrodynamics. The Gibbs relation for the surface phase (assumed to be two-parametric like fluid I) has the usual form

$$\mathrm{d}u_v^s = T \, \mathrm{d}S_v^s + \mu^s \, \mathrm{d}\rho^s. \tag{10}$$

Here u_v^s and S_v^s are the internal energy and the entropy per unit area; and μ^s is the surface chemical potential. Defining the non-convective entropy fluxes in the bulks and the interface as the ratios $\mathbf{J}_q^\pm / T$ and $\mathbf{J}_q^s / T$, respectively, we obtain from [9], [10], [7], [6] and [5] the following entropy balance equation:

$$\frac{\mathrm{d}^s S_v^s}{\mathrm{d}t} = -S_v^s \operatorname{div} \mathbf{v}^s - \operatorname{div}\left(\frac{\mathbf{J}_q^s}{T}\right) - \left(\frac{\mathbf{J}_{q,n}^+}{T} - \frac{\mathbf{J}_{q,n}^-}{T}\right) - S_v^+ (v_n^+ - v_n^s) + \sigma^s, \tag{11}$$

where

$$\sigma^s = \mathbf{J}_q^s \cdot \operatorname{grad} \frac{1}{T} + \frac{1}{T} (\mathbf{P}^s + p^s \mathbf{I}) : \operatorname{grad} \mathbf{v}^s + \frac{1}{2T} \mathbf{n} \cdot (\mathbf{P}^+ + \mathbf{P}^-) \cdot (\mathbf{I} - \mathbf{nn}) \cdot (\mathbf{v}_\parallel^+ - \mathbf{v}_\parallel^-)$$
$$+ \frac{1}{T} \rho^+ (v_n^+ - v_n^s) \left(\mu^s - \mu^+ + \frac{1}{\rho^+} \mathbf{n} \cdot \mathbf{P}'^+ \cdot \mathbf{n} \right) - \frac{1}{T} \mathbf{n} \cdot (\mathbf{P}^+ - \mathbf{P}^-) \cdot (\mathbf{I} - \mathbf{nn})$$
$$\cdot \left[\mathbf{v}_\parallel^s - \frac{1}{2} (\mathbf{v}_\parallel^+ + \mathbf{v}_\parallel^-) \right]. \tag{12}$$

Here σ^s is the surface entropy production; μ^+ and $\mathbf{P}'^+ = \mathbf{P}^+ + p^+\mathbf{I}$ are the chemical potential and the viscous stress tensor of fluid I, respectively; $\mathbf{I}$ is the metric tensor; and the subscript $\|$ denotes the component of the vector parallel to the interface. The surface pressure p^s, which is equal to the negative surface tension, is assumed to be related to the surface chemical potential in the usual way: $\rho^s\mu^s = u_v^s - TS_v^s + p^s$.

Representing the right-hand side of [12] as a sum of thermodynamic flux–force pairs and using the usual approach of irreversible thermodynamics (de Groot & Mazur 1962), we can construct linear relations linking the thermodynamic fluxes and forces. Obviously, this approach is valid close to equilibrium; the conditions of its applicability must be determined experimentally. Being interested in the principal effects which follow from our approach, we neglect all the cross-coefficients.

The last term of [12] defines the parallel component of $\mathbf{v}^s$:

$$\mathbf{v}_\parallel^s = \tfrac{1}{2}(\mathbf{v}_\parallel^+ + \mathbf{v}_\parallel^-) + \alpha \operatorname{div} \mathbf{P}^s \cdot (\mathbf{I} - \mathbf{nn}). \tag{13}$$

The coefficient α characterizes the influence of the surface pressure gradient on the velocity of the mass transport along the interface.

The first term on the right-hand side of [12] defines the Fourier law on the surface. This term is of no interest for the isothermal motion discussed below. Taking into account the two-dimensional isotropy of the surface and the isotropy in the bulk, we obtain from the next three terms of [12] that

$$\mathbf{P}^s = -p^s(\mathbf{I} - \mathbf{nn}) + \lambda^s(\operatorname{div} \mathbf{v}^s)(\mathbf{I} - \mathbf{nn}) + 2\eta^s(\mathbf{I} - \mathbf{nn}) \cdot \mathbf{E}^s \cdot (\mathbf{I} - \mathbf{nn}), \tag{14}$$

$$\tfrac{1}{2}\mathbf{n} \cdot (\mathbf{P}^+ + \mathbf{P}^-) \cdot (\mathbf{I} - \mathbf{nn}) = \beta(\mathbf{v}_\parallel^+ - \mathbf{v}_\parallel^-) \tag{15}$$

and

$$\rho^+(v_n^+ - v_n^s) = k_\rho\left[\mu^s(p^s, T) - \mu^+(p_0^+, T) + \frac{1}{\rho^+}\mathbf{n} \cdot \mathbf{P}_0^+ \cdot \mathbf{n}\right]. \tag{16}$$

Here λ^s and η^s are the "surface" viscosity coefficients; β is the coefficient of sliding friction (Bedeaux *et al.* 1976); k_ρ is the coefficient of the interface–bulk mass exchange; $\mathbf{E}^s = (\operatorname{grad} \mathbf{v}^s)^{\text{symm}}$ is the surface rate-of-strain tensor; and p_0^+ is the pressure of the fluid in the absence of motion.

Now let us carry out an order-of-magnitude analysis representing the interface as a layer of finite thickness. For this purpose, it is reasonable to assume that the viscosity coefficients in the layer are of the same order as those in the bulk. Comparing the last two terms on the right-hand side of [14] with the first one, we obtain that their ratios have the order of $\mathrm{Ca} \cdot h/L$, where $\mathrm{Ca} = \mu \cdot U/\sigma$ is the capillary number and h, L, μ, U and σ are the layer thickness [$\approx 10^{-9}$ to 10^{-8} m (Rowlinson & Widom 1982, pp. 174 and 181)], the characteristic length of velocity changes, the shear viscosity, the characteristic velocity and the surface tension, respectively. For macroscopic L and $\mathrm{Ca} \leqslant 1$, it is evident that $\mathrm{Ca} \cdot h/L \ll 1$ and the surface phase is "ideal" in the hydrodynamic sense, i.e.

$$\mathbf{P}^s = -p^s(\mathbf{I} - \mathbf{nn}). \tag{17}$$

Using [8], [15] and [17], we obtain a generalization of the no-slip boundary condition:

$$\mathbf{n} \cdot \mathbf{P}'^+ \cdot (\mathbf{I} - \mathbf{nn}) - \tfrac{1}{2}\operatorname{grad} p^s = \beta(\mathbf{v}_\parallel^+ - \mathbf{v}_\parallel^-). \tag{18}$$

Obviously, this boundary condition eliminates the shear-stress singularity of the classical solution. Applying [18] to the liquid–solid interface, we see that it relates the surface tension gradient with apparent slip without violation of the no-slip condition of the interface side facing the solid (Fig. 2). Representing again the interface as a layer of finite thickness and assuming that the slip coefficient β is of order μ/h, we find that the ratio of the first and the last terms of [18] has the order $h/L \ll 1$ everywhere except the immediate vicinity of the three-phase interaction region, which is discussed below. Thus, in the absence of the surface tension gradient, the shear friction could cause apparent slip of a liquid on a solid surface only at a distance of order h ($\sim 10^{-9}$ to 10^{-8} m) from the contact line. Far from the contact line, if the surface tension gradient is absent, [18] becomes the usual

no-slip boundary condition, $\mathbf{v}_\parallel^+ = \mathbf{v}^-$. Equation [18] without the second term is often used in conventional models for the contact-line motion on smooth and rough surfaces. However, it is necessary to emphasize that in applications with rough surfaces [18] without the second term is a result of averaging and therefore the slip coefficient β has another meaning and can be calculated by a purely hydrodynamic consideration (Hocking 1976). In section 7 we will discuss a very natural way of combining the approach of Hocking with the present one for surfaces of arbitrary roughness.

The second term in [18] has the order $(\delta p^s)/L_\sigma$, where L_σ is the characteristic length corresponding to surface tension changes of order δp^s. It is evident that this term may be comparable with the right-hand side of [18] for reasonable values of L_σ. Indeed, for example, if $\delta p^s \sim 10^{-2}$ to $10^{-1}\,\mathrm{N \cdot m^{-1}}$, $U \sim 10^{-2}\,\mathrm{m \cdot s^{-1}}$, $\mu \sim 10^{-3}\,\mathrm{Pa \cdot s}$ and $h \sim 10^{-9}$ to $10^{-8}\,\mathrm{m}$, one obtains $L_\sigma \sim 10^{-6}$ to $10^{-4}\,\mathrm{m}$.

The following remarks concerning the estimates given above should be noted. As will be shown below, we do not require any fixed degree of relative slip and of p^s deviation from its equilibrium value. Both quantities depend on the contact-line speed and change according to the conditions formulated below. Thus, the L_σ obtained above could be used only as a preliminary estimate of its order of magnitude (the upper limit).

The second remark concerns the value of β used for the order-of-magnitude analysis. According to some experiments with very thin films, the value of μ therein seems to be considerably greater than that in the bulk. Taking this into account, one could obtain a smaller value of L_σ than is given above.

Equation [16] determines the mass exchange between the bulk and the surface phase. For simplicity in the isothermal case considered here we will use the linear equation of state which reflects the main effect, i.e. changes of the surface pressure due to the surface density deviations from the value obtained in the absence of the non-symmetric influence of the bulks:

$$p^s = \gamma(\rho^s - \rho_0^s). \qquad [19]$$

A possible generalization of this equation will be discussed below. Equation [19] allows us to define the equilibrium surface density ρ_e^s by the equality

$$\mu^s(p^s(\rho_e^s), T) = \mu^+(p_0^+, T). \qquad [20]$$

Now the chemical potentials difference $\mu^s - \mu^+$ in [16] close to equilibrium may be approximately rewritten in the following way:

$$\mu^s - \mu^+ = \frac{\mathrm{d}\mu^s}{\mathrm{d}\rho^s}(\rho_e^s)(\rho^s - \rho_e^s). \qquad [21]$$

The last term in the square brackets on the right-hand side of [16] describes the mass flux into (or out of) the surface phase due to the liquid motion. We assume that this mass flux is negligible in comparison with the one caused by the deviation of the surface density from its equilibrium value. The corresponding criterion could be easily written but, as long as the value of $\mathrm{d}\mu^s/\mathrm{d}\rho^s$ is unknown, it would have a rather formal character. More details concerning this assumption and the order-of-magnitude analysis can be found elsewhere (Shikhmurzaev 1993a). Obviously, the solutions of the simplified model will belong to the set of solutions of the general model.

Introducing the parameter

$$\tau = \frac{1}{k_\rho \dfrac{\mathrm{d}\mu^s}{\mathrm{d}\rho^s}(\rho_e^s)}, \qquad [22]$$

and taking into account [16], [19]–[22] and the simplifications mentioned above, we may finally rewrite [5] as

$$\frac{\partial \rho^s}{\partial t} + \mathrm{div}\,\rho^s \mathbf{v}^s = -\frac{\rho^s - \rho_e^s}{\tau}. \qquad [23]$$

The parameter τ, called the surface tension relaxation time, characterizes the interval of time required for the interfacial structure formation (but not for the attachment of molecules to the

solid) and, in this sense, the present model generalizes that of Huh & Mason (1977). The idea of interfacial layer formation due to the mass flux from the bulk into the liquid–solid interfacial layer has been developed by Blake & Haynes (1969) also, based on the equations of chemical kinetics. However, Blake & Haynes did not consider the problem of the shear-stress singularity.

It is evident that for a non-singular surface density the surface–bulk mass exchange may be neglected in the boundary conditions for the bulk equations.

3. FORMULATION OF THE PROBLEM

Let us distinguish the following two asymptotic regions:

- The "outer" region (region 1, figure 1), where the classical solution (Moffatt 1964) with the no-slip boundary condition on the solid and the zero tangential stress on the free surface,

$$\mu_0 = \frac{1}{r}\frac{\partial \psi_0}{\partial \theta}, \quad v_0 = -\frac{\partial \psi_0}{\partial r} \qquad [24]$$

with

$$\psi_0 = \frac{r}{\sin\theta_d \cdot \cos\theta_d - \theta_d}[(\theta - \theta_d)\sin\theta - \theta\cos\theta_d \cdot \sin(\theta - \theta_d)],$$

is valid [the solution is represented in a dimensionless form, ψ is the stream function; u, v are, respectively, the radial and the transversal components of the velocity in a co-ordinate frame moving with the contact line; (r, θ) are polar co-ordinates in the plane of motion, defined such that the origin is at the contact line and the solid surface is in the plane $\theta = 0$; hereafter, the subscript 0 denotes parameters of the classical solution].

- The "slip" region (region 2, figure 1) with characteristic dimension $l \sim U\tau$, where the surface tension changes (and, therefore, slip) take place. In this region interfaces can be considered as geometrical surfaces of zero thickness and [8], [13], [17]–[19] and [23] are valid for the description of the surface parameter distributions. In comparison with l the dimensions of the three-phase interaction region in the plane of the flow may be neglected and this region considered as a point (the projection of the "contact line" to the plane of the flow).

The solutions of the Stokes equations in these two regions must be asymptotically matched as the ratio of l to the macroscopic length L tends to zero ($\epsilon = l/L \to 0$). Below we consider only the terms of $O(1)$ as $\epsilon \to 0$ and for these terms the matching procedure is very simple (see [30]).

Let us consider the boundary conditions for the Stokes equations in the "slip" region. We will use low indices 1 and 2 to mark the surface parameters of the gas–liquid and solid–liquid interface,

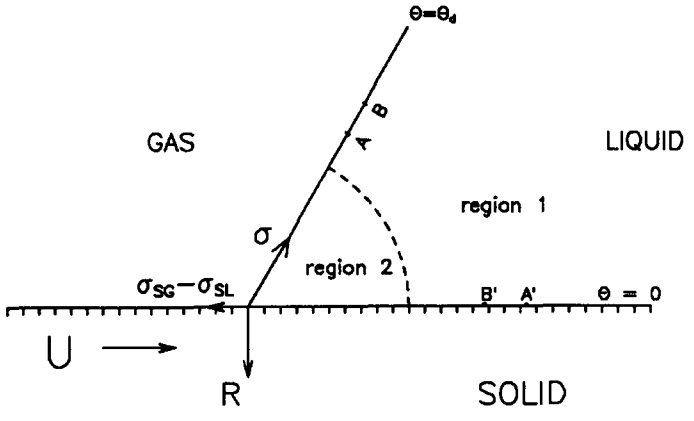

Figure 1. A general sketch for the flow perpendicular to the contact line and the force balance.

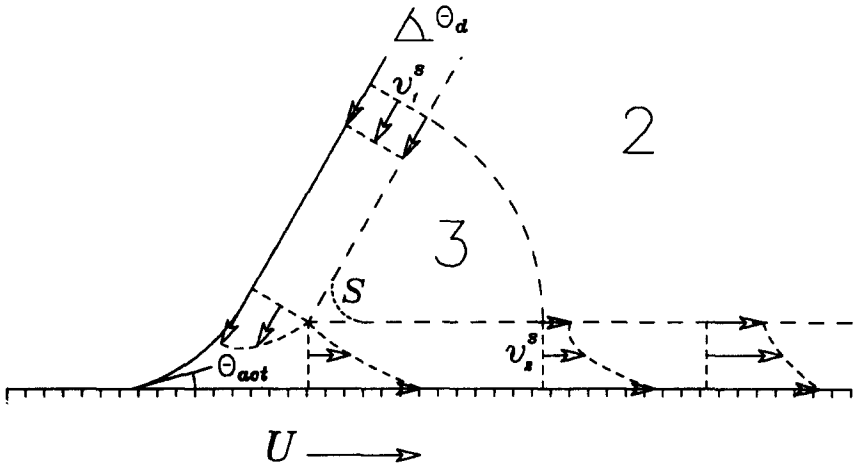

Figure 2. A detailed sketch for the flow in the immediate vicinity of the contact line. Region 3 has characteristic dimensions of $O(\mathrm{Ca})$. The interfaces are depicted as layers of finite thickness in order to show schematically the velocity distribution across the interface. The velocity on the side of the interfacial layer facing the liquid tends to that of the solid as the distance from the contact line increases. The actual slip is absent everywhere except for in the three-phase interaction region (i.e. the "contact line").

respectively. It is convenient to make the variables dimensionless using the following characteristic parameters: ρ_0^s (the surface density which corresponds to the zero surface pressure, see [19]); $\sigma = -p^s(\rho_{1e}^s)$ (the equilibrium tension of the gas–liquid interface); U (the speed of the solid in the chosen co-ordinate frame) and; $l = U\tau$ (the characteristic length of the surface tension relaxation).

Making use of [13], [17] and [19], for the stationary contact-line motion we may rewrite equations [23], [18] and the tangential projection of [8] for the gas–liquid interface as follows:

$$\frac{\mathrm{d}\rho_1^s v_1^s}{\mathrm{d}r} = -(\rho_1^s - \rho_{1e}^s), \qquad [25]$$

$$\frac{\mathrm{d}\rho_1^s}{\mathrm{d}r} = 4V^2(u(r, \theta_d) - v_1^s) \qquad [26]$$

and

$$\mathrm{Ca}\frac{1}{r}\frac{\partial u}{\partial \theta}(r, \theta_d) + \lambda\frac{\mathrm{d}\rho_1^s}{\mathrm{d}r} = 0, \qquad [27]$$

where

$$\mathrm{Ca} = \frac{\mu U}{\sigma}, \quad \lambda = \frac{\gamma\rho_0^s}{\sigma}, \quad V^2 = \frac{\tau\beta U^2}{\sigma\lambda(1+4A)}, \quad A = \alpha\beta.$$

Here λ is the characteristic compressibility of the liquid and V is the dimensionless contact-line speed. If the flow in the surface phase is imagined as a combination of the Couette and Poiseuille flows in a plane channel (see figure 2), the parameter A characterizes the relevance of such an analogy: for the channel flow $A = 1/12$.

For the solid–liquid interface [23], [18] and [13] take the form

$$\frac{\mathrm{d}\rho_2^s v_2^s}{\mathrm{d}r} = -(\rho_2^s - \rho_{2e}^s), \qquad [28]$$

$$\frac{2\mathrm{Ca}}{\lambda(1+4A)}\frac{1}{r}\frac{\partial u}{\partial \theta}(r, 0) - \frac{\mathrm{d}\rho_2^s}{\mathrm{d}r} = 4V^2(v_2^s - 1) \qquad [29]$$

and

$$u(r, 0) = 2v_2^s - 1 + \frac{2A}{(1+4A)V^2}\frac{\mathrm{d}\rho_2^s}{\mathrm{d}r}.$$

The solutions in the "slip" and "outer" regions must be matched and so

$$\rho_1^s \to \rho_{1e}^s, \quad u(r, \theta_d) \to u_0(\theta_d), \quad \rho_2^s \to \rho_{2e}^s, \quad u(r, 0) \to 1 \quad \text{as } r \to \infty. \tag{30}$$

Furthermore, we have the mass balance equation at the contact line,

$$\rho_1^s(0) v_1^s(0) + \rho_2^s(0) v_2^s(0) = 0, \tag{31}$$

which links the mass fluxes into and out of the contact-line region. If the surface is prewetted or the *precursor* film takes place, [31] must be modified in a manner which takes into account the additional mass flux into the contact-line region (Shikhmurzaev 1993b).

To find the dynamic contact angle value we must consider the force balance at the contact line. In statics the contact angle θ_s is related to the tangential projections of forces acting on the contact line by Young's equation, which can be written in terms of surface pressures as

$$p^s(\rho_{1e}^s)\cos\theta_s = p_{SG}^s - p^s(\rho_{2e}^s). \tag{32}$$

The parameter $\sigma_{SG}(= -p_{SG}^s)$ is the surface tension of the gas–solid interface (Young 1805). An alternative interpretation of p_{SG}^s and a possible method of its measurement are discussed below. Equation [32] implies that the vertical component of the force acting along the gas–liquid interface is always balanced by a reaction force from the solid (figure 1).

Considering the tangential projection of momentum of the contact line and neglecting the inertial components of the momentum fluxes as before, we may write the generalized Young's equation as

$$p^s(\rho_1^s(0))\cos\theta_d = p_{SG}^s - p^s(\rho_2^s(0)), \tag{33}$$

where the surface pressure and surface densities are connected by [19].

Now we can formulate the moving contact-line problem for small Re and Ca in the following way. If the bulk pressure is made dimensionless using the quantity μ/τ, the velocity and the pressure in the bulk obey the (dimensionless) Stokes equations,

$$\operatorname{div} \mathbf{u} = 0, \quad \nabla p = \Delta \mathbf{u}, \tag{34}$$

and satisfy [25]–[31] and [33]. The static contact angle is related to the quantities involved in the boundary conditions by [32].

Taking the projection of [8] tangential to the solid surface, we obtain that the (dimensionless) density of the force acting on the solid

$$f_t = -\frac{dp^s}{dr} + \mathrm{Ca}\,\frac{1}{r}\frac{\partial u}{\partial \theta}(r, 0). \tag{35}$$

4. SMALL Ca

The consideration of [25]–[34] is rather difficult and here we will discuss only the case of small Ca. As Ca→0, the system [25]–[34] becomes singularly perturbed and its solution can be found using singular perturbation methods. The *outer* solution is valid in the region which we will call "intermediate", since in our terminology the "outer" region (region 1, figure 1) is the one associated with the classical solution [24]. The "intermediate" region occupies the major part of the "slip" region and below we will assume for simplicity that this region is shown in figures 1 and 2 as region 2.

The *inner* solution of [25]–[34] is valid in region 3 (figure 2), referred to below as the "inner" or "viscous" region. The inner variable is $\tilde{r} = r/\mathrm{Ca}$. Below we consider only the main terms of asymptotic expansions in Ca as Ca→0.

In the "intermediate" region we may neglect the terms proportional to Ca in [27]. Integrating [25]–[27] and using the matching conditions [30], we obtain

$$\rho_1^s = \rho_{1e}^s, \quad u(r, \theta_d) \equiv v_1^s(r) \equiv u_0(\theta_d). \tag{36}$$

Thus, the surface density and, consequently, the surface pressure of the gas–liquid interface have their equilibrium values up to the "inner" region. The interface velocity is equal to the radial

velocity of the classical solution at $\theta = \theta_d$, $u_0(\theta_d)$. It can be shown that the next terms of the interface density and the surface velocity asymptotic expansions, as Ca$\to$0, have the orders Ca $\cdot$ ln(Ca) and Ca, respectively.

Equations [28] and [29] in the "intermediate" region take the form

$$\frac{d\rho_2^s v_2^s}{dr} = -(\rho_2^s - \rho_{2e}^s), \quad \frac{d\rho_2^s}{dr} = 4V^2(1 - v_2^s) \tag{37}$$

and

$$u(r, 0) = 2v_2^s - 1 + \frac{2A}{(1+4A)V^2}\frac{d\rho_2^s}{dr}. \tag{38}$$

It is convenient to rewrite the last two matching conditions [30] in an equivalent form:

$$\rho_2^s \to \rho_{2e}^s, \quad v_2^s \to 1 \quad \text{as } r \to \infty. \tag{39}$$

Let us consider the "inner" region, marking all the variables there with a tilde ($\tilde{}$) and using the inner independent variable $\tilde{r} = r/\text{Ca}$. From [25]–[29], we immediately obtain that

$$\tilde{\rho}_1^s, \tilde{\rho}_2^s, \tilde{v}_1^s, \tilde{v}_2^s = \text{const}, \tag{40}$$

i.e. the main terms of the asymptotic expansions in Ca of $\tilde{\rho}^s$ and $\tilde{v}^s$ are independent of $\tilde{r}$. Taking this into account and using the matching conditions in the form

$$\lim_{\tilde{r}\to\infty} \tilde{\phi} = \lim_{r\to 0} \phi, \tag{41}$$

we come to the conclusion that [31] and [33] are valid for the inner limits of the solution in the "intermediate" region. Making use of [36] and [24], we may rewrite [31] as

$$\rho_2^s(0)v_2^s(0) = -\rho_{1e}^s u_0(\theta_d), \quad u_0(\theta_d) = \frac{\sin\theta_d - \theta_d\cos\theta_d}{\sin\theta_d\cos\theta_d - \theta_d}. \tag{42}$$

Thus, the dynamic contact angle may be calculated from [37], [42], [33], [39] and [19], which may be rewritten in dimensionless form as

$$p^s = \lambda(\rho^s - 1). \tag{43}$$

We remind the reader that the constants ρ_{1e}^s, ρ_{2e}^s, ρ_{SG}^s and θ_s are related by [32].

Now let us consider the force f $(= -f_t)$ experienced by the liquid. Neglecting the term proportional to Ca in [35], we see that in the "intermediate" region the tangential component of the force density equals the surface pressure gradient

$$f(r) = \frac{dp^s}{dr}(\rho_2^s(r)). \tag{44}$$

In the "inner" region $\tilde{f} = O(1)$ as Ca$\to$0 and both terms on the right-hand side of [35] are of the same order. The matching condition [41] gives $f(0) = \tilde{f}(\infty)$ and the total tangential force calculated with the help of the uniformly valid expansion

$$F = \int_0^\infty \left[f(r) + \tilde{f}\left(\frac{r}{\text{Ca}}\right) - \tilde{f}(\infty)\right] dr = p^s(\rho_{2e}^s) - p^s(\rho_2^s(0)) + O(\text{Ca}) \quad \text{as Ca}\to 0.$$

Using [32] and [33], taking into account that dimensionless $p^s(\rho_{1e}^s) = -1$ and neglecting the terms of order Ca, we may rewrite the expression for F as

$$F = \cos\theta_s - \cos\theta_d. \tag{45}$$

It is an interesting result, since the relationship [45] often used in the analysis of wetting phenomena as an additional *empirical* condition is *derived theoretically* on the basis of the present approach. This derivation makes clear the conditions of applicability of [45].

Thus, we may conclude that in the framework of the present approach the macroscopic characteristics of the advancing contact-line motion (the dynamic contact angle and the force experienced by the liquid) in the case of low Ca can be calculated from [37], [42], [33], [39], [43],

i.e. using only the solution in the "intermediate" region. We should point out that in the present model the *actual* slip does not occur, since the velocity of the interface side facing the solid surface is equal to the velocity of the solid. This property of the model is in complete agreement with the results obtained by molecular-dynamics simulations (Koplik *et al.* 1988, 1989; Thompson & Robbins 1989). These studies show that the "no-slip boundary condition broke down within ~ 2 atomic spacing from the contact line" (Thompson & Robbins 1989), i.e. in the three phase-interaction region (the "contact line"), if we translate this assertion into the thermodynamic language used here.

It is necessary to make a special remark about the pressure singularity. In the classical solution [24] the pressure singularity is not integrable and has the form $p \sim 1/r$. If one eliminates the shear-stress singularity, introducing in some way the slip boundary condition, the pressure becomes integrable, $p \sim \ln(r)$, but the singularity still remains. This singularity exists, since the surface which bounds the flow domain, i.e. the region where the Stokes equations are used, is not smooth. The idealized model, consisting of the flow domain with simple geometry and the slip boundary condition eliminating the bulk velocity discontinuity at the edge, is convenient for a mathematical consideration but it leads to the appearance of the stagnation point at the edge of the "bulk" as well as to the pressure singularity. Obviously, in the vicinity of the three-phase interaction zone (i.e. the "contact line") one may choose the surface separating the "interface" and the "bulk" in different ways and, in general, this surface should be smooth, e.g. the surface S in figure 1. Using the mass and momentum balance equations in the integral form, we could easily show that in the case of small Ca for any *regular* boundary conditions on a *smooth* surface S the pressure singularity and the stagnation point disappear, but the macroscopic parameters of the advancing liquid are still determined by the *same* system, [37], [42], [33], [39] and [43], which describes the distribution of surface quantities in the *intermediate* region. This is a very essential feature of the present model. Thus, bearing in mind this remark, we may use the approach developed for the modelling of wetting phenomena.

It is necessary to note that, in contrast to conventional models, our approach guarantees that the fluid motion is *rolling* [see feature (i) in section 1]: it is an immediate consequence of [42] which binds the mass fluxes into and out of the contact-line region.

We must point out also that in a general case, the θ_d considered here is not equal to either the *actual* (θ_{act}, figure 2) or the *apparent* contact angle. The latter is formed by the solid surface and the free surface far from the contact line. As has been shown by Ngan & Dussan (1982), the *apparent* contact angle depends on the measuring device, while the angle introduced here is a characteristic of the wetting process and is independent of the manner of its measurement. We will call θ_d the *macroscopic* dynamic contact angle to distinguish it from the *actual* and *apparent* angles. It is necessary to mention that (1) the macroscopic contact angle alone is the boundary condition for the hydrodynamic equation which describes the free surface shape and (2) in many experiments just the *macroscopic* contact angle was measured.

5. ANALYSIS

In this section we investigate the properties of the problem [37], [42], [33], [39] and [43]. As was shown in the previous section, the macroscopic properties of the advancing contact-line motion can be obtained from the system of *ordinary* differential equations [37] with boundary conditions [42], [33], [39] and [43] and the equality [45] defining the force between the liquid and the solid. The characteristics of the bulk flow are present implicitly through the radial velocity of the free surface $u_0(\theta_d)$ (see [42]). The obtained value of θ_d defines the flow domain and [38] gives the distribution $u(r, 0)$, which together with $u(r, \theta_d)$ $(= u_0(\theta_d)$, see [36]) sets the boundary conditions for the Stokes equations [34] which describe the flow field in the "intermediate" region.

The solution of [37], [42], [33], [39] and [43] depends on four dimensionless parameters: ρ^s_{1e}, V, p^s_{SG} and θ_s (p^s_{2e} is replaced by θ_s with the help of [32]). The dimensionless surface density ρ^s_{1e} characterizes the "rarefaction" of a liquid at a gas–liquid interface. To carry out the order-of-

magnitude analysis it is convenient to represent the interface as a layer of finite thickness h, assuming that

$$\sigma \sim p \cdot h, \quad p \sim \left(\frac{\partial p}{\partial \rho}\right)_T \cdot (\rho - \rho_0), \quad \rho^s \sim \rho \cdot h.$$

Using the values (Daniels & Alberty 1975; Moelwyn–Hughes 1961)

$$\sigma \sim 10^{-2} \text{ to } 10^{-1}\ \mathrm{N \cdot m^{-1}}, \quad h \sim 10^{-9} \text{ to } 10^{-8}\ \mathrm{m},$$

$$\left(\frac{\partial p}{\partial \rho}\right)_T \sim (1 \text{ to } 2) \cdot 10^6\ \mathrm{m^2 \cdot s^{-2}}, \quad \rho_0 \sim 10^3\ \mathrm{kg \cdot m^{-3}},$$

we have $1 - \rho^s_{1e} \sim 5 \cdot (10^{-4} \text{ to } 10^{-2})$. The expression for the dimensionless speed V shows that in wetting phenomena there is a specific characteristic contact-line speed:

$$U_{CL} = \left[\frac{\sigma\lambda(1+4A)}{\tau\beta}\right]^{1/2} = \left[\frac{\gamma\rho^s_0(1+4\alpha\beta)}{\tau\beta}\right]^{1/2}.$$

It is interesting that U_{CL} is determined only by the properties of the spreading liquid and is independent of the characteristics of the media which are in contact with the liquid in the vicinity of the contact line. The parameter U_{CL} is of order $1\text{–}10^2 \cdot \mathrm{m \cdot s^{-1}}$.

Thus, the parameter V depends only on the properties of the liquid, ρ^s_{1e} is a function of the gas–liquid pair while θ_s and p^s_{SG} are determined by the materials of the three contacting media.

The system [37], [42], [33], [39] and [43] was solved numerically using the fourth-order Runge–Kutta method. The results are presented in figures 3–7 and 9–13.

Let us consider the case $p^s_{SG} = 0$. The role and physical interpretation of this parameter when it is not zero will be discussed later. If $p^s_{SG} = 0$, the horizontal component of the force exerted on the contact line from the free surface is entirely balanced by the surface pressure of the solid–liquid interface (see [32] and [33]). In figure 3 we present the dependence of the dynamic contact angle on the dimensionless contact-line speed V for different values of ρ^s_{1e}. We remind the reader that $\lambda = \rho^s_0\gamma/\sigma = 1/(1-\rho^s_{1e})$. Curves 1, 2 and 3 correspond to $\rho^s_{1e} = 0.95$, 0.99 and 0.999, respectively. To illustrate the influence of the other parameters, in the following we will fix the value of ρ^s_{1e}, say $\rho^s_{1e} = 0.99$. As $V \to \infty$, $\theta_d \to \theta_{max} = 180°$ and $\rho^s_2(0) \to \rho^s_{1e}$.

Figure 4 shows the dependence of θ_d on V for different static contact angles. These curves describe the evolution of θ_d for the liquid spreading over different solids for which the limitation $p^s_{SG} = 0$ is valid. In this case the limiting contact angle value is $\theta_{max} = 180°$, independent of θ_s. Such $\theta_d(V)$ dependence is typical for most gas–liquid–solid systems (Inverarity 1969; Hoffman 1975; Ström *et al.* 1990).

Typical distributions of the tangential force density f acting on the fluid obtained from [44] are shown in figure 5. As expected, the force density increases as the contact-line speed grows. Equation [45] and the dependences shown in figure 4 describe the velocity dependences of θ_d and the total tangential force F for different θ_s *without* any empirical adjustable functions.

Recent results of Zhou & Sheng (1990), obtained for two different models with slip on the solid surface, show that in the case of small Ca the difference between the *macroscopic* (in our sense) and *apparent* contact angles is negligible and, since experiments reveal considerable deviations of the measured contact angles from the static values, this fact must be attributed to the dependence of the *macroscopic* contact angle on the contact-line speed. However, this dependence is usually ignored in theoretical studies. Zhou & Sheng (1990) also used [45] as an *additional* condition to calculate the force between the liquid and the solid. In our model the dependence of the macroscopic contact angle on the contact-line speed is obtained in a natural way, and [45] is *derived* theoretically.

Now let us consider the case $p^s_{SG} \neq 0$. The parameter $\sigma_{SG} = -p^s_{SG}$ in Young's theory characterizes the surface tension of a gas–solid interface. However, one can "measure" only the difference

$$\sigma_{SG} - \sigma_{SL} = p^s(\rho^s_2) - p^s_{SG}$$

by substituting measured values of $p^s(\rho^s_{1e})$ and θ_s into [32]. It is necessary to emphasize that Young's equation contains the forces acting on the contact line and σ_{SG} is not equal to the true "surface tension of the solid".

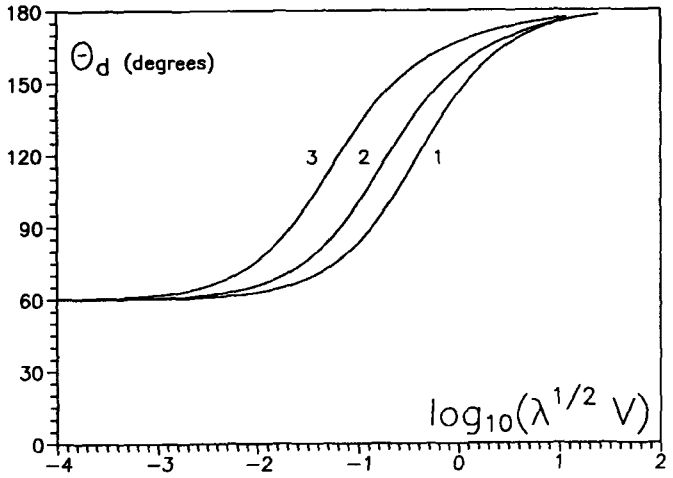

Figure 3. Dependence of the dynamic contact angle on the dimensionless contact-line speed for different degrees of the surface phase "rarefaction". Curves 1, 2, 3 correspond to $\rho^s_{1e} = 0.95$, 0.99 and 0.999, respectively; $p^s_{SG} = 0$, $\theta_s = 60°$. We remind that $\lambda = 1/(1 - \rho^s_{1e})$.

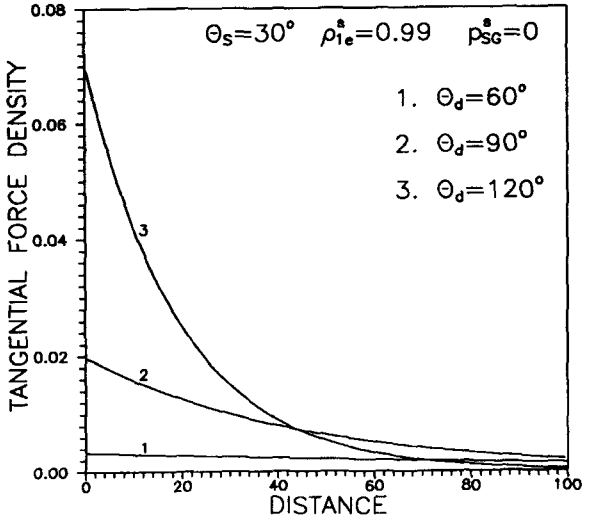

Figure 5. Distribution of the tangential force density.

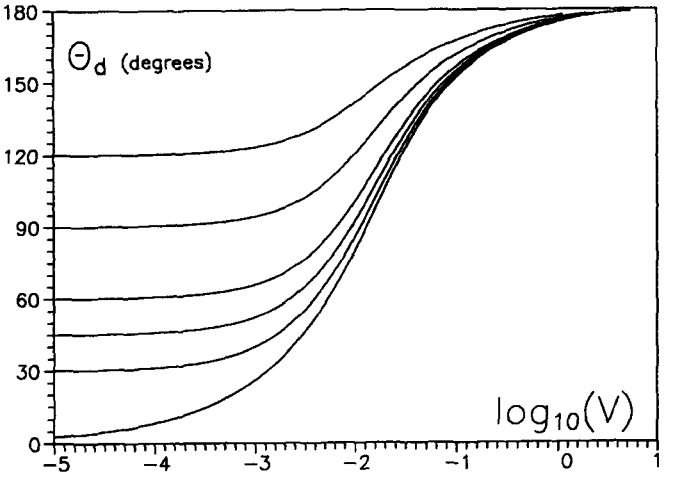

Figure 4. Dynamic contact angle vs dimensionless contact-line speed for different values of the static contact angle; $\rho^s_{1e} = 0.99$, $p^s_{SG} = 0$.

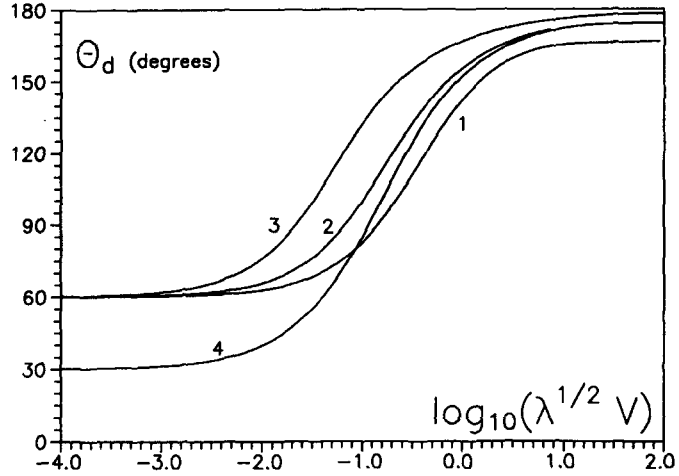

Figure 6. Dynamic contact angle vs dimensionless contact-line speed for $p^s_{SG} < 0$: **1**—$\rho^s_{1e} = 0.95$, $\theta_s = 60°$, $p^s_{SG} = -0.5$; **2**—$\rho^s_{1e} = 0.99$, $\theta_s = 60°$, $p^s_{SG} = -0.5$; **3**—$\rho^s_{1e} = 0.999$, $\theta_s = 60°$, $p^s_{SG} = -0.5$; **4**—$\rho^s_{1e} = 0.99$, $\theta_s = 30°$, $p^s_{SG} = -0.5$.

We are able to propose a method which allows us, at least in principle, to obtain p^s_{SG} from dynamic experiments. Indeed, calculations show (figure 6) that p^s_{SG} determines the value of θ_{max}. If $p^s_{SG} < 0$, θ_{max} becomes $< 180°$ and sensitive to the value of ρ^s_{le} but remains independent of θ_s. A limiting contact angle value of $< 180°$ was observed in some gas–liquid–solid systems (Ablett 1923; Elliott & Riddiford 1967; Schwartz & Tejada 1972).

Experiments (Elliott & Riddiford 1967; Schwartz & Tejada 1972) show that $\theta_{max} < 180°$ can be obtained by a proper choice of the *whole* gas–liquid–solid system and the major role belongs to the liquid–solid pair and not to the gas–solid one. Thus, p^s_{SG} may be interpreted as a tangential component of the reaction force acting on the contact-line region from a solid. This component depends on the nature of all the contacting materials.

Figure 6 shows that θ_{max} is a function of ρ^s_{le} and p^s_{SG}. Since ρ^s_{le} is a property of the gas–liquid interface only, it can be measured independently. Thus, if $\theta_{max} < 180°$, we may suppose that $p^s_{SG} < 0$ and use the value of θ_{max} to determine p^s_{SG}.

It is necessary to emphasize, however, that if the solid surface is prewetted, θ_{max} becomes considerably less than 180°, even for positive p^s_{SG}. The detailed analysis of this case can be found elsewhere (Shikhmurzaev 1993b).

A number of experiments (Burley & Kennedy 1976a, b; Blake & Ruschak 1979; Gutoff & Kendrick 1982) show that at a certain contact-line speed the spreading of a liquid on a solid surface becomes unstable: the contact line takes a "sawtooth" form and air entrainment begins. Usually the air entrainment occurs at $\theta_d = 180°$. In this connection let us consider the properties of the model for $p^s_{SG} > 0$ (figure 7). Calculations show that, if $p^s_{SG} > 0$, the system [37], [42], [33], [39] and [43] has a maximum speed of wetting V_*, so that for $V > V_*$ the solution of the problem fails to exist. As $V = V_*$, $\theta_d = 180°$. If the velocity of the solid is greater than V_*, the contact line must change its form to make the normal component of the velocity equal to V_*. Thus, the contact-line form becomes "sawtooth". For the first time, the existence of a maximum contact-line speed and its connection with changes in the contact-line form and air entrainment were considered by Blake & Ruschak (1979).

Calculations show (figure 7) that V_* is independent of the "rarefaction" of the liquid at a gas–liquid interface, $(1 - \rho^s_{le})$, and decreases as the absolute value of p^s_{SG} increases. An augmentation of θ_s decreases the value of V_* as well. It is interesting to note that for certain values of ρ^s_{le} and p^s_{SG} the curve θ_d (log V) has a practically rectilinear region. The same regions (with the same inclinations) are present in experimental curves (Gutoff & Kendrick 1982). However, it is difficult to carry out a quantitative comparison of theoretical results with these experimental data. Indeed, the theoretical curves depend on two parameters, ρ^s_{le} and p^s_{SG}, unknown in this experiment and on the value of $\log(Ca) - \log(V)$, which links the theoretical and experimental dimensionless

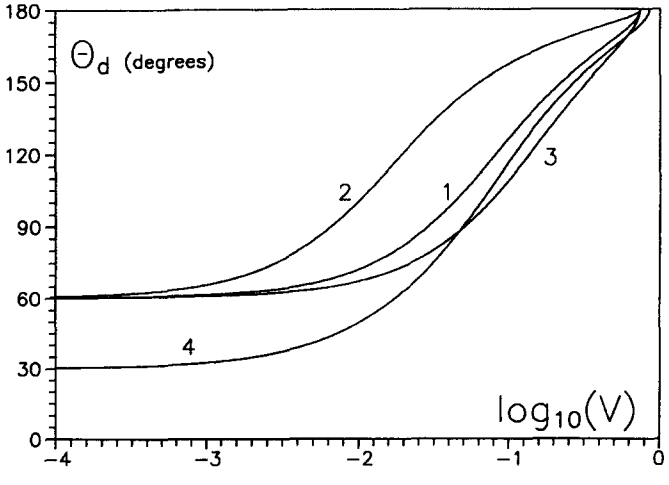

Figure 7. Dynamic contact angle vs dimensionless contact-line speed for $p^s_{SG} > 0$: **1**—$\rho^s_{le} = 0.95$, $\theta_s = 60°$, $p^s_{SG} = 0.5$; **2**—$\rho^s_{le} = 0.99$, $\theta_s = 60°$, $p^s_{SG} = 0.5$; **3**—$\rho^s_{le} = 0.9$, $\theta_s = 60°$, $p^s_{SG} = 0.5$; **4**—$\rho^s_{le} = 0.95$, $\theta_s = 30°$, $p^s_{SG} = 0.5$.

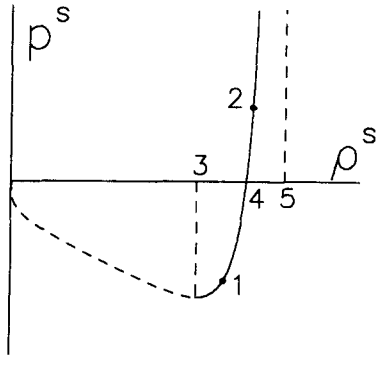

Figure 8. Possible generalization of the $p^s(\rho^s)$ dependence: **1**—$(\rho^s_{le}, p^s(\rho^s_{le}))$; **2**—$(\rho^s_{2e}, p^s(\rho^s_{2e}))$; **3**—$\rho^s_{min}$; **4**—$\rho^s_0$; **5**—$\rho^s_{max}$.

velocities (see section 6). Since these unknown parameters strongly (and in different ways) influence the shape of the theoretical curve in the (Ca, θ_d) co-ordinate plane and the value of V_*, any quantitative comparison of the theory with these experiments will not seem convincing. At the present time we may only state that our theory is in good qualitative agreement with these experiments.

It is worth mentioning that the existence of a maximum contact-line speed is possible in the $p^s_{SG} < 0$ case as well. In this case, as V increases, $\rho^s_2(0)$ changes from ρ^s_{2e} to a certain value $\rho^s_{2\min} < \rho^s_{1e}$. If the interface is rarefied so that ρ^s becomes less than ρ^s_{1e}, the equation of state [19] may become inapplicable and should be altered in a way which allows one to take into account the fact that the surface tension of the interface is bounded. A possible variant of $p^s(\rho^s)$ dependence is shown in figure 8. Calculations with a $p^s(\rho^s)$ dependence of this type give that, if $p^s_{SG} < 0$, at a certain value of $V = V_{**}$ the surface pressure $p^s(\rho^s_2(0))$ reaches the minimum of the curve $p^s(\rho^s)$ and for $V > V_{**}$ a solution of the problem fails to exist. The dynamic contact angle value which corresponds to V_{**} is $< 180°$, though, if the deviation of θ_d from 180° is small, it is rather difficult to detect it experimentally.

6. COMPARISON WITH EXPERIMENTAL DATA

As was noted in the previous section, the quantitative comparison of theoretical and experimental results for $p^s_{SG} \neq 0$ requires independent measurement (direct or indirect) of a number of parameters. However, it is possible to carry out a preliminary comparison of experiments and theory. In some works, experimenters have reported on the asymptotic behaviour of the dynamic contact angle as the contact-line speed grows. If θ_d asymptotically tends to 180°, we may conclude that $p^s_{SG} = 0$ and use the corresponding theoretical curve for the experimental data description. Besides this, it is necessary to mention that, if the values of $|p^s_{SG}|$ and/or $|1 - \rho^s_{1e}|$ are small, the deviation of $\theta_d(\log V)$ from the corresponding curve obtained for $p^s_{SG} = 0$ becomes considerable only for θ_d close to 180°. Thus, to describe experimental data in this case and reduce the number of adjustable parameters, we may also use the dependence $\theta(\log(V))$ calculated for $p^s_{SG} = 0$.

Furthermore, analysis of experiments [see Dussan (1979) for a review] as well as theoretical models shows that besides the parameters of the classical model we must introduce some additional, intrinsic, parameters (e.g. the slip length, the relaxation time etc.) which are important for the moving contact-line description. Consequently, the system of dimensionless similarity parameters of the classical model *is not complete* and the attempts to represent all the experimental data by a single empirical correlation associated with this system, say $\theta_d(\mathrm{Ca}, \theta_s)$ (Inverarity 1969; Hoffman 1975), seems unfounded *in principle*. Some contradictions of such representations were pointed out by Dussan (1979). Thus, the experimental dependence of θ_d on Ca must be interpreted as the dependence of θ_d on the dimensionless contact-line speed. The dimensionless speed V introduced in the present paper is related to Ca by

$$V = \mathrm{Ca} \cdot \mathrm{Yu}; \quad \mathrm{Yu} = \left[\frac{\sigma\tau\beta}{\lambda\mu^2(1+4A)}\right]^{1/2}. \qquad [46]$$

The transition from co-ordinates $(\log(V), \theta_d)$ to $(\log(\mathrm{Ca}), \theta_d)$ corresponds to the shift of a curve by log(Yu). We know that, as $p^s_{SG} = 0$, changes in ρ^s_{1e} lead to analogous shifts in the theoretical curve $\theta_d(\log(V))$ (see figure 3). Thus, we may fix the value of ρ^s_{1e} (say, $\rho^s_{1e} = 0.99$) and use the parameter log(Yu) to try to fit the theoretical curve to the experimental data. To verify the possibility of describing the *whole* experimental *curve* using *one constant* log(Yu), experiments in which the variation of θ_d is large are chosen. A comparison of the theory with a number of experiments was carried out and, taking into account the same general behaviour of the experimental curves, in figures 9–12 we present the results of such a comparison for the well-known experimental data of Hoffman (1975) and the recent results of Ström *et al.* (1990). The values of the parameters for the theoretical curves are given in figure captions. As is clear from this comparison, the theoretical curves are in good agreement with the experimental data.

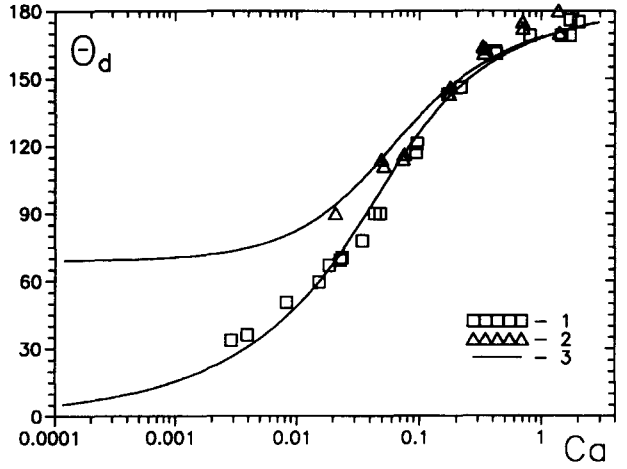

Figure 9. Comparison of the theory with experimental data for the advancing interface in a glass capillary (Hoffman 1975): **1**—Brookfield std viscosity fluid, $\theta_s = 0°$; **2**—Admex 760, $\theta_s = 69°$; **3**—theoretical curves ($p^s_{SG} = 0$, $\rho^s_{le} = 0.99$): log(Yu) = −0.45 (**1**) and −0.55 (**2**).

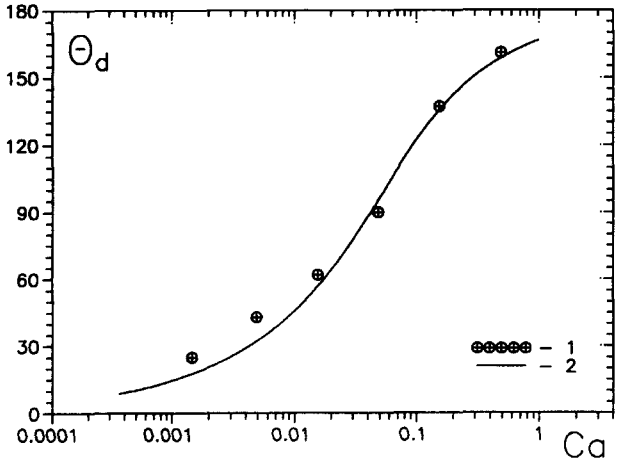

Figure 11. Comparison of the theory (**2**) with the experimental data (**1**) obtained using the entering tape technique (silicone oil 2/oxidized polystyrene) by Ström *et al.* (1990), $\theta_s = 0°$. Theoretical curve: $p^s_{SG} = 0$, $\rho^s_{le} = 0.99$; log(Yu) = −0.5.

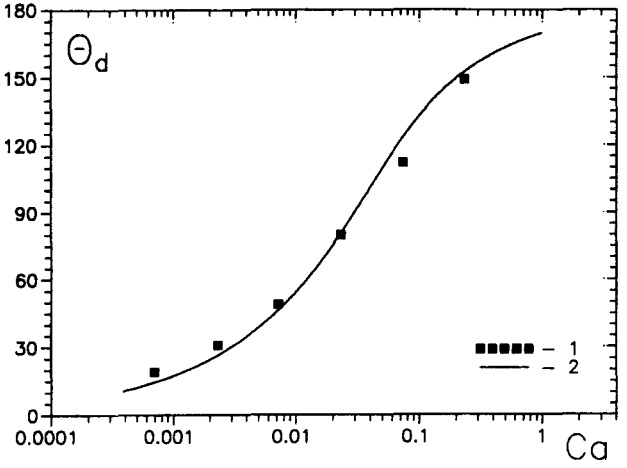

Figure 10. Comparison of the theory (**2**) with the experimental data (**1**) obtained using the tape (untreated polystyrene) entering a bath of silicone oil 1 (Ström *et al.* 1990), $\theta_s = 0°$. Theoretical curve: $p^s_{SG} = 0$, $\rho^s_{le} = 0.99$; log(Yu) = −0.35.

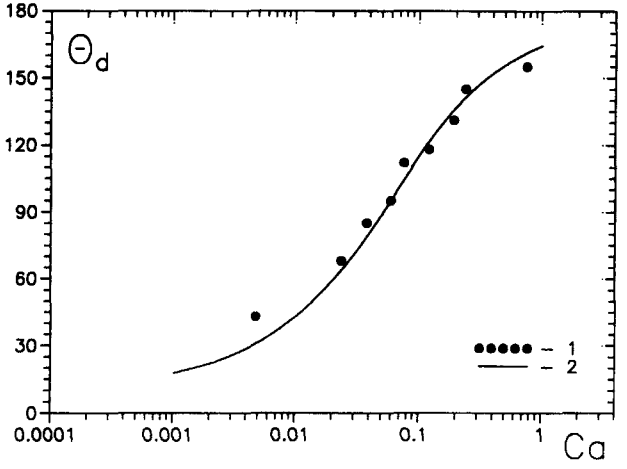

Figure 12. Comparison of the theory (**2**) with the experimental data (**1**) obtained using the entering tape technique (silicone oil 3/untreated polystyrene) by Ström *et al.* (1990), $\theta_s = 12°$. Theoretical curve: $p^s_{SG} = 0$, $\rho^s_{le} = 0.99$; log(Yu) = −0.6.

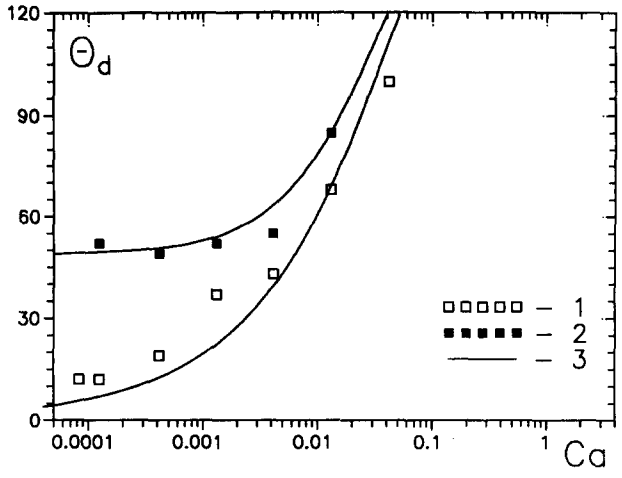

Figure 13. Experimental data (Ström *et al.* 1990) of paraffin oil spreading on different solids (1—untreated polystyrene, $\theta_s = 0°$; 2—polytetrafluoroethylene, $\theta_s = 49°$) are described theoretically (3) using one and the same value of $\log(\mathrm{Yu}) = -0.25$ ($p^s_{SG} = 0$, $\rho^s_{le} = 0.99$).

Let us use another indirect way of testing the theory. The parameter Yu depends only on the properties of the liquid and of the gas–liquid interface (see [46]), and it is possible to fix this parameter by matching the theory with one of the experiments in the manner described above. Then, we may consider the spreading of the same liquid over another solid and see if the theory describes this experiment with the same value of Yu. The results of such testing show that it is really so (figure 13).

It is necessary to point out that the second method of testing requires the estimation of the surface roughness effects, since otherwise a non-systematic experimental error may occur.

Summing up the results presented in figures 9–13, we may come to the preliminary conclusion that the theory developed in the present paper is in good agreement with experiments performed on different solids using different liquids over a wide range of parameters.

7. DISCUSSION

As was shown in the previous sections, in the case of small Ca and Re the flow itself causes the surface tension gradient along the liquid–solid interface which strongly influences the flow and determines its macroscopic parameters. This effect may be called the self-induced Marangoni effect. The model based on the surface tension relaxation analysis:

—eliminates the singularity of the shear stress inherent in the classical solution and allows us to calculate the force acting between a solid and a liquid which spreads on its surface;
—is in agreement with direct experimental observations describing the fluid motion as *rolling*;
—gives the contact angle dependence on the contact-line speed;
—explains the existence of the limiting contact angles $< 180°$;
—predicts the existence of the maximum contact-line speed and, consequently, the conditions of the incipient air entrainment.

In section 2 we pointed out some common features between the physical background of the present theory and the works of Blake & Haynes (1969) and Huh & Mason (1977). Now let us compare the different theories from a formal mathematical point of view. The description of wetting phenomena requires the consideration of the Stokes (or Navier–Stokes) equations in the flow domains with piecewise smooth boundaries. In order to remove the shear-stress singularities at the edges, the conventional boundary conditions must be altered so that slippage near the moving contact lines can take place. However, the problem is that not only the shear stress but the shape of the flow domain is velocity dependent and, in addition to the classical boundary conditions

describing evolution of the smooth parts of the boundary, a theory for the contact angle dependence on the contact-line speed is required. Thus, an approach aimed only at the elimination of the shear-stress singularity is forced to use an additional, adjustable function—the dependence of the *macroscopic* (in our terminology) contact angle on the contact-line speed. Most existing theories postulate that the *macroscopic* dynamic contact angle is equal to the static one, independent of the contact-line speed. This assumption allows us to pose and solve mathematical problems associated with wetting processes but, as was shown by Zhou & Sheng (1990), is in conflict with experimental observations. The advantage of the present theory is that it describes both the velocity dependence of the apparent slip distribution and the contact angle evolution *without* any adjustable functions in the framework of a self-consistent approach based on a certain physical background.

Now we will discuss the main assumptions which have been used in constructing the model and some possible ways for its generalization. In the derivation of the equations describing the process of interface formation we have used the simplest variant of Onsager's approach, in which the cross effects are neglected and the proportionality coefficients between the thermodynamic forces and fluxes are constant. We have also used additional simplifications—neglecting the mass exchange between the interface and the bulk due to the fluid motion and replacing the real equation of state for the surface phase by the linear one. Abandoning these simplifications, taking into account the dependence of Onsager's coefficients on the constitutive parameters and taking into consideration the cross-effects as well as the possible non-isothermal character of the process, we could obtain a number of more and more generalized models. However, such a generalization should be a consequence of the experimental verification of the simplest model which, as was shown in the present paper, is sufficient to describe the main features of the phenomenon. It is necessary to emphasize that Onsager's approach itself is valid only in the case when the deviations of the parameters from their equilibrium values are not "too large", and the conditions for its applicability must be determined experimentally as well.

It is interesting to note that the problem [37], [42], [33], [39] and [43] could be easily reformulated for a non-Newtonian fluid. Indeed, the fluid rheology is manifested only by the function $u_0(\theta_d)$, which represents the solution of the classical problem. If $u_0(\theta_d)$ is replaced by the corresponding function of the "outer" flow of a non-Newtonian fluid, we could describe the spreading of this fluid on a solid surface. We remind the readers that in our model the interfaces are "ideal" in the hydrodynamic sense.

It is noteworthy that conventional models developed on the basis of a purely macroscopic consideration of the solid surface roughness (Hocking 1976) could be combined with the present approach in a very natural way. According to this combination, the whole physical picture of wetting is as follows. If the solid surface is smooth, a liquid spreads over it in accordance with the model presented here. As the surface roughness increases, the present model begins to describe the wetting of surface roughness elements and the dynamic contact angle calculated here begins to deviate from the one formed by the gas–liquid interface and the "effective" plane surface of the solid. A further increase in the solid roughness and the speed of liquid spreading leads to the situation in which the speed of "wetting" due to the surface roughness (Hocking 1976) becomes greater than the one obtained here. In this case, the *macroscopic* picture of wetting is described by the model of Hocking (within the microscopic contact angle equal to θ_d obtained in the present paper), while the present model remains valid for the description of the wetting of surface roughness elements at and behind the "front" of macroscopic "wetting". Thus, the new model presented here, being applicable to smooth solid surfaces, could be combined with conventional models of "wetting" due to the surface roughness and lead, at least in principle, to a model suitable for solid surfaces of arbitrary roughness.

REFERENCES

ABLETT, R. 1923 An investigation of the angle of contact between paraffin wax and water. *Phil. Mag.* **46**, 244–256.

ADAM, N. K. 1930 *The Physics and Chemistry of Surfaces*. Clarendon Press, Oxford.

BAIOCCHI, C. & PUKHNACHEV, V. V. 1990 Problems with one-sided limitations for Navier–Stokes equations and the dynamic contact angle problem. *J. Appl. Mech. Technol. Phys. (U.S.S.R.)* **2,** 27–40.

BASCOM, W. D., COTTINGTON, R. L. & SINGLETERRY, C. R. 1964 Dynamic surface phenomena in the spontaneous spreading of oils on solids. In *Contact Angle, Wettability and Adhesion; Advances in Chemistry*, Vol. 43, pp. 355–379. Am. Chem. Soc., Washington, DC.

BATCHELOR, G. K. 1967 *An Introduction to Fluid Dynamics*. Cambridge Univ. Press, U.K.

BEDEAUX, D., ALBANO, A. M. & MAZUR, P. 1976 Boundary conditions and non-equilibrium thermodynamics. *Physica* **A82,** 438–462.

BLAKE, T. D. & HAYNES, J. M. 1969 Kinetics of liquid/liquid displacement. *J. Colloid Interface Sci.* **30,** 421–423.

BLAKE, T. D. & RUSCHAK, K. J. 1979 A maximum speed of wetting. *Nature* **282,** 489–491.

BOENDER, W., CHESTERS, A. K. & VAN DER ZANDEN, A. J. J. 1991 An approximate analytical solution of the hydrodynamic problem associated with an advancing liquid–gas contact line. *Int. J. Multiphase Flow* **17,** 661–676.

BURLEY, R. & KENNEDY, B. S. 1976a An experimental study of air entrainment at a solid/liquid/gas interface. *Chem. Engng Sci.* **31,** 901–911.

BURLEY, R. & KENNEDY, B. S. 1976b A study of the dynamic wetting behavior of polyester tapes. *Br. Polym. J.* **8,** 140–143.

COX, R. G. 1986 The dynamics of the spreading of liquids on a solid surface. Part 1. Viscous flow. *J. Fluid Mech.* **168,** 169–194.

DANIELS, F. & ALBERTY, R. A. 1975 *Physical Chemistry*, 4th edn. Wiley, New York.

DEFAY, R. & PRIGOGINE, I. 1966 *Surface Tension and Absorbtion*. Longmans & Green, London.

DURBIN, P. A. 1988 Consideration on the moving contact line singularity with application to frictional drag on a slender drop. *J. Fluid Mech.* **197,** 157–169.

DUSSAN, V. E. B. 1976 The moving contact line: the slip boundary condition. *J. Fluid Mech.* **77,** 665–684.

DUSSAN, V. E. B. 1979 On the spreading of liquids on solid surfaces: static and dynamic contact lines. *A. Rev. Fluid Mech.* **11,** 371–400.

DUSSAN, V. E. B. & DAVIS, S. H. 1974 On the motion of a fluid–fluid interface along a solid surface. *J. Fluid Mech.* **65,** 71–95.

ELLIOTT, G. E. P. & RIDDIFORD, A. C. 1967 Dynamic contact angles. I. The effect of impressed motion. *J. Colloid Interface Sci.* **23,** 389–398.

DE GENNES, P. G. 1985 Wetting: statics and dynamics. *Rev. Mod. Phys.* **57,** 827–863.

DE GENNES, P. G., HUA, X. & LEVINSON, P. 1990 Dynamics of wetting: local contact angles. *J. Fluid Mech.* **212,** 55–63.

GREENSPAN, H. P. 1978 On the motion of a small viscous droplet that wets a surface. *J. Fluid Mech.* **84,** 125–143.

DE GROOT, S. R. & MAZUR, P. 1962 *Non-equilibrium Thermodynamics*. North-Holland, Amsterdam.

GUTOFF, E. B. & KENDRICK, C. E. 1982 Dynamic contact angles. *AIChE Jl* **28,** 459–466.

HARDY, W. B. 1919 The spreading of fluids on glass. *Phil. Mag.* **38,** 49–55.

HESLOT, F., CAZABAT, A.-M. & LEVINSON, P. 1989 Dynamics of wetting of tiny drops: ellipsometric study of the late stages of spreading. *Phys. Rev. Lett.* **62,** 1286–1288.

HOCKING, L. M. 1976 A moving fluid interface on a rough surface. *J. Fluid Mech.* **76,** 801–817.

HOCKING, L. M. 1977 A moving fluid interface. Part 2. The removal of the force singularity by a slip flow. *J. Fluid Mech.* **79,** 209–229.

HOCKING, L. M. & RIVERS, A. D. 1982 The spreading of a drop by capillary action. *J. Fluid Mech.* **121,** 425–442.

HOFFMAN, R. 1975 A study of the advancing interface. I. Interface shape in liquid–gas systems. *J. Colloid Interface Sci.* **50,** 228–241.

HUH, C. & MASON, S. G. 1977 The steady movement of a liquid meniscus in a capillary tube. *J. Fluid Mech.* **81,** 401–419.

HUH, C. & SCRIVEN, L. E. 1971 Hydrodynamic model of steady movement of a solid/liquid/fluid contact line. *J. Colloid Interface Sci.* **35,** 85–101.

INVERARITY, G. 1969 Dynamic wetting of glass fibre and polymer fibre. *Br. Polym. J.* **1,** 245–251.

KOPLIK, J., BANAVAR, J. R. & WILLEMSEN, J. F. 1988 Molecular dynamics of Poiseuille flow and moving contact lines. *Phys. Rev. Lett.* **60,** 1282–1285.

KOPLIK, J., BANAVAR, J. R. & WILLEMSEN, J. F. 1989 Molecular dynamics of a fluid flow at solid surfaces. *Phys. Fluids* **A1,** 781–794.

LAMB, H. 1932 *Hydrodynamics*. Dover, New York.

LOWNDES, J. 1980 The numerical simulation of the steady movement of a fluid meniscus in a capillary tube. *J. Fluid Mech.* **101,** 631–645.

MOELWYN-HUGHES, E. A. 1961 *Physical Chemistry*. Pergamon Press, Oxford.

MOFFATT, H. K. 1964 Viscous and resistive eddies near a sharp corner. *J. Fluid Mech.* **18,** 1–18.

NEOGI, P. & MILLER, C. A. 1976 Spreading kinetics of liquids on rough solid surfaces. *J. Colloid Interface Sci.* **56,** 460–468.

NGAN, C. G. & DUSSAN, V. E. B. 1982 On the nature of the dynamic contact angle: an experimental study. *J. Fluid Mech.* **118,** 27–40.

NGAN, C. G. & DUSSAN, V. E. B. 1989 On the dynamics of liquid spreading on solid surfaces. *J. Fluid Mech.* **209,** 191–226.

ROWLINSON, J. S. & WIDOM, B. 1982 *Molecular Theory of Capillarity*, pp. 174, 181. Clarendon Press, Oxford.

SCHONHORN, H., FRISCH, H. L. & KWEI, T. K. 1966 Kinematics of wetting of surfaces by polymer melts. *J. Appl. Phys.* **17,** 4967–4973.

SCHWARTZ, A. M. & TEJADA, S. B. 1972 Studies of dynamic contact angles on solids. *J. Colloid Interface Sci.* **38,** 359–375.

SHIKHMURZAEV, Y. D. 1993a A two-layer model of an interface between immiscible fluids. *Physica* **A192,** 47–62.

SHIKHMURZAEV, Y. D. 1993b Dynamic contact angles in gas/liquid/solid systems and the flow field in the vicinity of a moving contact line. To be published.

STRÖM, G., FREDRIKSSON, M., STENIUS, P. & RADOEV, B. 1990 Kinetics of steady-state wetting. *J. Colloid Interface Sci.* **134,** 107–115.

THOMPSON, P. A. & ROBBINS, M. O. 1989 Simulation of contact line motion: slip and the dynamic contact angle. *Phys. Rev. Lett.* **63,** 766–769.

VOINOV, O. V. 1976 Hydrodynamics of wetting. *Fluid Dynam.* **11,** 714–721.

VOINOV, O. V. 1978 Asymptote to the free surface of a viscous liquid creeping on a surface and the velocity dependence of the angle of contact. *Soviet Phys. Dokl.* **23,** 891–893.

YARNOLD, G. D. 1938 The motion of a mercury index in a capillary tube. *Proc. Phys. Soc. Lond.* **50,** 540–552.

YOUNG, T. 1805 An essay on the cohesion of fluids. *Phil. Trans. R. Soc. Lond.* **95,** 65–87.

ZHOU, M. Y. & SHENG, P. 1990 Dynamics of immiscible fluid displacement in a capillary tube. *Phys. Rev. Lett.* **64,** 882–885.